

# Fast magnetization switching of Stoner particles: A nonlinear dynamics picture

Z. Z. Sun and X. R. Wang

*Physics Department, The Hong Kong University of Science and Technology, Clear Water Bay, Hong Kong SAR, China*

(Dated: June 20, 2018)

The magnetization reversal of Stoner particles is investigated from the point of view of nonlinear dynamics within the Landau-Lifshitz-Gilbert formulation. The following results are obtained. 1) We clarify that the so-called Stoner-Wohlfarth (SW) limit becomes exact when damping constant is infinitely large. Under the limit, the magnetization moves along the steepest energy descent path. The minimal switching field is the one at which there is only one stable fixed point in the system. 2) For a given magnetic anisotropy, there is a critical value for the damping constant, above which the minimal switching field is the same as that of the SW-limit. 3) We illustrate how fixed points and their basins change under a field along different directions. This change explains well why a non-parallel field gives a smaller minimal switching field and a short switching time. 4) The field of a ballistic magnetization reversal should be along certain direction window in the presence of energy dissipation. The width of the window depends on both of the damping constant and the magnetic anisotropy. The upper and lower bounds of the direction window increase with the damping constant. The window width oscillates with the damping constant for a given magnetic anisotropy. It is zero for both zero and infinite damping. Thus, the perpendicular field configuration widely employed in the current experiments is not the best one since the damping constant in a real system is far from zero.

PACS numbers: 75.60.Jk, 75.75.+a, 05.45.-a

## I. INTRODUCTION

Magnetic data storage is one of the important components of modern computers. Data input and output involve switching the magnetization of magnetic storage cells (magnetization reversal). The typical switching time with currently used technology is of order of nanosecond. If one wants to have a faster computer (modern electronic computers are working at a clock speed of order of GHz), the conventional magnetization reversal method shall soon (the clock speed is doubled every year in the past) become a bottleneck. Thus fast magnetization switching shall be of great importance for the future development of high speed information industry.

The reversal of a magnetization can be achieved in many different ways, and it is a very complicated issue[1]. For example, in a bulk material, the magnetization reversal can go through bucking and curling modes, or nucleation and domain formation. The recent advance of technology allows us to fabricate the magnetic nano-particles that are believed to be useful for high density information storage[2, 3, 4, 5]. For a magnetic nano-particle, the magnetic moments of all atoms are normally aligned in the same direction, creating a so-called single magnetic domain. Such a nano-particle is usually called a Stoner-Wohlfarth or Stoner particle. The understanding of magnetization reversal of a single magnetic domain should be relatively simple in comparison with that in a bulk system, but important in nano-technologies[6].

There are two challenging issues about magnetization reversal. One is how to have a short reversal time, and the other is how to make the switching field to be small.

The conventional magnetization reversal technique is to apply a magnetic field antiparallel to the initial magnetization. A large enough field can drive the initial state out of local minimum and at the same time make the target state to be the global minimum. Thus the system can roll down to the target state through ringing effect[7, 8, 9]. For the issue of minimal switching field, the classical result, called Stoner-Wohlfarth (SW) limit, was given by Stoner and Wohlfarth[10].

Recently picoseconds magnetization switching has been observed in experiments[11, 12] by using pulse magnetic fields. Unlike the conventional method, the magnetic field is applied in a perpendicular direction such that the magnetization undergoes a precession. This approach has also received many theoretical attentions[13, 14, 15, 16]. Numerical investigations[13] showed that the switching time can be substantially reduced because ringing effect can be suppressed so that the magnetization will move along a so-called ballistic trajectory[16]. The precessional magnetization reversal provides not only a shorter time but also lower switching field (well below the SW-limit), as found in the early numerical calculations[17]. In the absence of energy dissipation, precessional magnetization switching can also be investigated analytically. Analytical results for the minimal field were obtained by Porter[18]. Recently Xiao and Niu have also studied the minimal field required in the precessional magnetization switching in a conservative system[19]. Their results were based on fast switching such that the energy dissipation can be neglected and the magnetic system can be regarded as a conservative system. They used the phase plane to reveal the properties of magnetization reversal. It was shown that precessional

magnetic switching occurs when localized trajectories in phase plane become delocalized.

Although it is reasonable to approximate a Stoner particle as a conservative system in a short time if the damping (dissipation) during its dynamical motion is small. A real magnetic particle is not a truly conservative system when the damping is large or if one is interested in the long time behave. Dissipation should be taken into account and a Stoner particle should be treated as a non-conservative system. In this paper we re-examine the magnetization reversal as a nonlinear dynamical system in the presence of dissipation. The magnetic dynamics of a single domain magnetic particle can be described by the evolution trajectories in the phase plane. One can use the general concepts of nonlinear dynamics not only to understand all results from previous studies, but also to see the validity conditions of some of these results such as the SW-limit. The paper is organized as follows. In Sec. II we first reformulate the magnetization reversal in terms of nonlinear dynamics concepts, such as attractors and phase flow. Previous results are re-interpreted in such language. The Landau-Lifshitz-Gilbert (LLG) equation is introduced. Our main results are presented in Sec. III. The conditions under which the SW limit is valid are given. For a given magnetic anisotropy, we shall show that there is a critical damping constant above which the minimal switching field is the same as that of SW-limit. The reason and meaning of this critical damping constant are also given. The change of fixed points and their basins under a magnetic field is investigated. We show that the field corresponding to the ballistic reversal changes from the perpendicular direction for a conservative system to a direction window in the presence of energy dissipation. The conclusion is given in Section IV.

## II. A NONLINEAR DYNAMICS PICTURE OF MAGNETIZATION REVERSAL

### II.1 Attractors, phase flow and magnetization reversal

Previous results on the magnetization reversal of Stoner particles can be conveniently described in the terminology of nonlinear dynamics. The phase space related to the magnetization is a two dimensional (2D) plane because all atomic magnetic-moments are aligned in the same direction, and the magnetization can rotate under an external and/or an internal effective magnetic field that can exert a torque on the spin. The polar angle  $\theta$  and the azimuthal angle  $\phi$ , shown in (Fig. 1a), can fully determine a magnetization  $\vec{m}$ . In the  $\theta - \phi$  plane, each point corresponds to a particular state of the magnetization. A state will in general evolve to new states due to its dynamics. Its motion can be described by a trajectory in the phase plane, called phase flow. The phase flow for

a dissipative system ends to a few types of destiny (attractors), including fixed points, limit cycles, or strange attractors. They correspond to stable states, periodic, aperiodic and chaotic motions[20]. In a 2D phase plane, however, strange attractor solution is not allowed.

The only attractor related to the magnetization reversal of Stoner particles is fixed points. The magnetization reversal problem is as follows: Before applying an external magnetic field, there are two stable fixed points (denoted by A and B in Fig. 1b), corresponding to magnetizations, say  $\vec{m}_0$  (point A) and  $-\vec{m}_0$  (point B), along its easy axis. The phase plane can be divided into two parts, called basins of attractors. One is around A, and the other around B, denoted by shadowed areas in Fig. 1b. The system in basin A(B) will end up at state A(B). Initially, the magnetization is  $\vec{m}_0$ , and the goal is to apply a small external field to switch the magnetization to  $-\vec{m}_0$  fast.

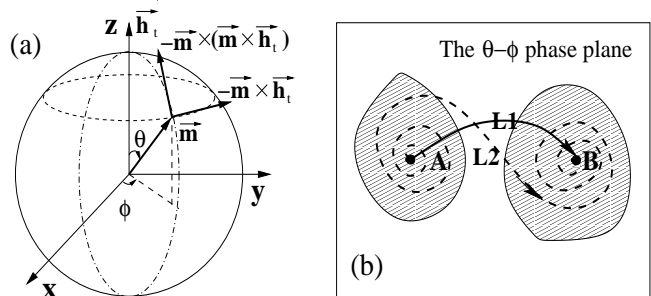


FIG. 1: (a) The magnetization  $\vec{m}$  can be uniquely determined by angles  $\theta$  and  $\phi$ .  $z$ -axis is assumed to be along the total magnetic field  $\vec{h}_t$ .  $-\vec{m} \times \vec{h}_t$  determines the precession direction, and  $-\vec{m} \times (\vec{m} \times \vec{h}_t)$  decides the dissipation direction. (b) The  $\theta - \phi$  phase plane for the magnetization of a Stoner particle. Point A and point B represent the initial and the target state, respectively. Two shadowed areas denote schematically basins of two stable fixed points A and B. The solid curve L1 and dashed curve L2 illustrate two different phase flow connected A and B.

### II.2 Damping and non-damping magnetization reversals

The conventional magnetization switching is based on a damping mechanism through, typically, the spin-lattice relaxation. From the point of view of nonlinear dynamics, the idea behind the method is to construct the external magnetic field in such a way that the target state is the only stable fixed point. In another word, basin A (Fig. 1b) is reduced to zero and the whole (except probably a few isolated points) phase plane is the target state basin (Basin B). The minimal reversal field (SW-limit) is the one at which basin A shrinks to a point. Since the initial and the target states have very large energy difference, the extra energy must be dumped into the lattice

during a spiral motion before the system reaches the final state. The system first spirals out of A, and then spirals toward B, denoted by phase flow L2 in Fig. 1b. This spiral motion is often referred[16] to as ringing effect. The reversal time is largely determined by the effectiveness of energy dissipation.

On the other hand, the target state does not need to be the only fixed point in the recent fast magnetization switching. In fact, it does not even need to be a fixed point. In the precessional magnetization reversal, one applies a short magnetic field pulse such that both initial and final states are not fixed points, and system will start to flow in the phase plane. In order to switch the magnetization, one needs to let the system to reach the basin of the final state (Basin B) such that the system will flow to the target state after the pulse field is switched off. Ideally, one wants both initial and target states on its precessional path. This is a non-damping method, and the reversal time does not rely on the spin relaxation time. There are several ways with different control precisions to move the system to the desired state. One way is to apply a perpendicular pulse field to ‘kick’ the system to basin B. In comparison with conventional method, the spiral motion out of the initial state is replaced by a ballistic[16] motion. However, the system relies on ringing effect to reach the final state. It was shown[13] that the switching time can be reduced substantially, but it is still hundreds of picoseconds for a normal magnetic particle due to the ringing effect in the last stage of magnetization reversal.

The proposal of Xiao and Niu[19] is a fully ballistic magnetization reversal scheme. Neglecting the energy dissipation during the motion of a Stoner particle in a magnetic field, the magnetization must move on an equal potential line. Thus the idea is to apply an external magnetic field with a proper strength and in a right direction such that both the initial and the target states have the same energy and are on the same phase flow trajectory as schematically illustrated by the solid line L1 connected points A and B with an arrow in Fig. 1b. Without damping, there is no extra energy to dissipate in this new approach, thus the system move from the initial state to the final one in a ballistic way instead of in a ringing mode. The typical time for a precession of  $180^\circ$  in a field of teslas is order of picoseconds for usual magnetic materials so a picoseconds magnetic field pulse is required in this method. As soon as the system arrives at the target state, one needs to switch off the external field, so the target state becomes a fixed point of the system again. This approach thus requires a precise control of the pulse duration.

From computational point of view, the magnetization reversal time can be evaluated as soon as the phase flow connected the initial and the target states is found. The reversal time is given by the length  $dl$  of phase flow line

divided by the phase velocity  $\sqrt{\dot{\theta}^2 + \dot{\phi}^2}$  which is determined by the system dynamics,

$$t = \int_A^B \frac{dl(\theta, \phi)}{\sqrt{\dot{\theta}^2 + \dot{\phi}^2}}. \quad (1)$$

In the language of nonlinear dynamics, an external field modifies the dynamics by changing the phase velocity field. This velocity field is in general a continuous function of the external field. A phase flow between the initial and target states could only been set up when the external field is strong enough because the initial and final states are two stable fixed points with equally large basins at the beginning. The minimal switching field is the critical one at which such a flow is created.

### II.3 The Landau-Lifshitz-Gilbert equation

The magnetization dynamics of a Stoner particle is governed by the Landau-Lifshitz-Gilbert (LLG) equation[21],

$$\frac{d\vec{M}}{dt'} = -|\gamma|\vec{M} \times \vec{H}_t + \frac{\alpha}{M_s}\vec{M} \times \frac{d\vec{M}}{dt'},$$

which can also be written as

$$(1 + \alpha^2)\frac{d\vec{M}}{dt'} = -|\gamma|\vec{M} \times \vec{H}_t - \frac{\alpha|\gamma|}{M_s}\vec{M} \times (\vec{M} \times \vec{H}_t). \quad (2)$$

Here  $|\gamma| = 2.21 \times 10^5 (\text{rad/s}) / (A/m)$  is the gyromagnetic ratio,  $M_s$  is the saturated magnetization of the particle, and  $\alpha$  is the phenomenological dimensionless damping constant. The typical experimental values of  $\alpha$ [11] ranges from 0.037 to 0.22 for different Co films. The equation describes the motion of magnetization vector  $\vec{M}$  under an applied magnetic field  $\vec{H}$  in the presence of an arbitrary magnetic anisotropy energy density function  $W(\vec{M}, \vec{H})$ . The total field  $\vec{H}_t = -\nabla_{\vec{M}} W(\vec{M}, \vec{H}) / \mu_0 = \vec{H}_{eff} + \vec{H}$ , where  $\vec{H}_{eff}$  denotes the internal effective field due to the magnetic anisotropy.  $\mu_0 = 4\pi \times 10^{-7} N/A^2$  is the vacuum magnetic permeability.

It is convenient to write the LLG equation in a dimensionless form by defining  $\vec{m} \equiv \vec{M}/M_s$ , scaled field  $\vec{h}_t \equiv \vec{H}_t/M_s = \vec{h}_{eff} + \vec{h}$ , scaled time  $t \equiv t'/(|\gamma|M_s)$ , and  $w(\vec{m}, \vec{h}) \equiv W(\vec{M}, \vec{H})/(\mu_0 M_s^2)$ . The equation for  $\vec{m}$  becomes

$$(1 + \alpha^2)\frac{d\vec{m}}{dt} = -\vec{m} \times \vec{h}_t - \alpha\vec{m} \times (\vec{m} \times \vec{h}_t). \quad (3)$$

As shown in Fig. 1a, the first term in the right hand side of Eq. (3) describes the precession motion around the total field and the second term decides the dissipation direction toward the total field. In our analysis, we always use parameters of Co as our references. For Co film[11],

$M_s = 1.36 \times 10^6 A/m$ , thus the time unit is approximately  $3.33ps$  and the energy unit is  $2.32 \times 10^6 J/m^3$ .

In terms of  $\theta - \phi$ , the dynamics of the magnetization is determined by the following non-conservative two-dimensional nonlinear autonomous dynamical equations[16],

$$\begin{aligned} (1 + \alpha^2)\dot{\theta} &= -\alpha \frac{\partial w}{\partial \theta} - \frac{1}{\sin \theta} \frac{\partial w}{\partial \phi}, \\ (1 + \alpha^2)\dot{\phi} &= \frac{1}{\sin \theta} \frac{\partial w}{\partial \theta} - \frac{\alpha}{\sin^2 \theta} \frac{\partial w}{\partial \phi}. \end{aligned} \quad (4)$$

Different particles is characterized by different magnetic anisotropic energy density functions  $w(\vec{m}, \vec{h})$ . In our analysis, we always assume it to be the uniaxial with its easy axis along the x-direction. Due to the rotation symmetry around the easy axis, the applied field can be chosen in the x-z plane without losing generality. The general form of  $w(\vec{m}, \vec{h})$  can be written as

$$w(\vec{m}, \vec{h}) = f(m_x) - m_x h_x - m_z h_z, \quad (5)$$

where  $h_x$  and  $h_z$  are the applied magnetic field along x- and z-axis, respectively.

This naive-looking nonlinear dynamical equation does not have exact solutions yet. Analytical results can only be obtained in some special cases. For example, analytical solutions were found[22, 23] in the absence of the internal effective field ( $\vec{h}_{eff} = 0$ ). The analytical analysis can also be done if there is no energy dissipation as what is shown in Reference [18, 19]. In general, one can use the fourth-order Runge-Kutta method to study the system numerically. In this study, we will use following  $f(m_x)$  in Eq. (5) with different  $k_2$  and  $k_4$ , whenever we need to use numerical results to illustrate our understandings,

$$f(m_x) = -\frac{1}{2}k_2 m_x^2 - \frac{1}{4}k_4 m_x^4. \quad (6)$$

Here  $k_2, k_4$ , accounting for the strength of the anisotropy, are positive numbers. In the next section, we shall present our main findings.

### III. RESULTS AND DISCUSSIONS

#### III.1 The exactness of SW-limit at infinitely large dissipation

The conventional method is based on damping mechanism. Its classical result is the so-called SW-limit. For an uniaxial model with the easy axis along x-axis and magnetic field in xz-plane, the SW-limit is obtained by assuming that the magnetization moves in the xz-plane during its reversal. The minimal switching field is given

by[10]

$$\frac{dw}{dm_x} = 0, \quad (7)$$

$$\frac{d^2w}{dm_x^2} = 0, \quad (8)$$

with  $m_x^2 + m_z^2 = 1$ . For a widely studied case of  $k_2 \neq 0$  and  $k_4 = 0$ , the SW-limit[10] is

$$(h_x/k_2)^{2/3} + (h_z/k_2)^{2/3} = 1, \quad (9)$$

corresponding to the solid-line in Fig. 2. The SW-limits for various choices of  $k_4$  are also plotted in Fig. 2.

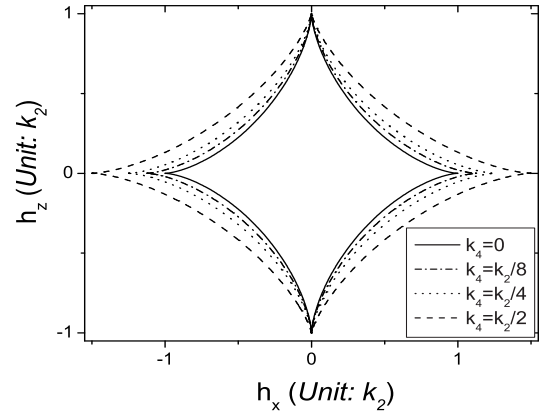


FIG. 2: The SW-limit for various choices of  $k_2, k_4$ . Solid curve:  $k_4 = 0$ ; dash-dot curve:  $k_4 = k_2/8$ ; dotted curve:  $k_4 = k_2/4$ ; dashed curve:  $k_4 = k_2/2$ .

The original SW-limit was derived in the static case[10]. As shown in the dynamical Eq. (3), the first term on the right hand side will lift the magnetization away from the xz-plane. Thus the assumption of the SW-limit that the magnetization moves in the xz-plane is only true when this term can be neglected. This will happen when damping constant becomes infinite ( $\alpha \rightarrow \infty$ ). In this case, the magnetization will move toward the total field as denoted by the big circle passing through the north-south poles in Fig. 1a. This is the steepest energy descent path for the magnetization. Thus, the minimal switching field of SW-limit corresponds to the one at which there is only one minimum in energy landscape.

#### III.2 Critical value of damping constant

In a realistic system, as damping constant is not infinitely large, the magnetization does not need to move along the steepest energy descent path. As a result, a system may still move from the initial state to the local minimum located near the target state even when an external field is smaller than the SW-limit. So, after

the external field is removed, the system will move toward the target state through a ringing mode, achieving the magnetization switching. As it was shown in many previous studies[17, 18], the minimal switching field can be smaller than the SW-limit. Numerical calculations[17] show that when the damping constant  $\alpha < 1$ , magnetization switching can occur well below the SW-limit. While  $\alpha \geq 1$ , the minimal switching field is the SW-limit. Thus, it implies a critical  $\alpha_c$  exists, above which the minimal switching field is given by the SW-limit. In Reference 17,  $\alpha_c = 1$ . To the best of our knowledge, there is no clear understanding of this result. In fact, previous studies[17] seem suggesting that  $\alpha_c = 1$  is very special. We want to show that there is indeed a critical damping constant for a given magnetic anisotropy. But, this critical value can be different for different anisotropy, and  $\alpha = 1$  is not special. We shall provide an explanation to the  $\alpha_c$ .

In order to understand the origin of the critical  $\alpha$ , let us consider energy landscape under different external field. As we mentioned in the previous section, there is only one stable fixed point when  $h > h_{SW}$ . Asymptotically, the system shall always end up at the fixed point for any non-zero damping. Thus, if one switch off the field after it reaches the fixed point, the system will surely move to the target state (state B). There is also a  $h_1 < h_{SW}$  at which the energy of system at the initial state equals that at the saddle point between two stable fixed points. Thus there is no way to switch the magnetization when  $h < h_1$  because the energy of the initial state (A) is too smaller to overcome the potential barrier between the initial and final states.  $h_1$  can be determined from the following equations

$$\frac{dw}{dm_x} = 0, \quad (10)$$

$$w(m_x) = w_A, \quad (11)$$

where  $w_A$  is the energy at the initial state ( $m_x = 1$ ). For a field  $h$  between  $h_1$  and  $h_{SW}$ ,  $h_1 < h < h_{SW}$ , there exist two stable fixed points with a saddle point in between. Furthermore, the energy of the initial state is higher than that of the saddle point. Fig. 3 is a schematic 3D plot of the energy landscape for the case of  $h_1 < h < h_{SW}$ . Point A denotes the initial state, whose energy is supposed to be higher than that of the saddle point (SP) between two local minima. In this case, the flow starting from A will finally evolve into either of two fixed points, depending on the value of  $\alpha$ . When  $\alpha$  is infinity, the system will evolve into the minimum near the initial state along the steepest descent path, as shown by line R1. For the opposite extreme of zero damping ( $\alpha = 0$ ), the system will move along an equal potential contour (line R4) surround the two minima (fixed points), as investigated in Reference 19. For small  $\alpha$ , the magnetization can make many turns around the two local minima before it falls into either one. So there is a special  $\alpha = \alpha_i$  with which the system just touches the

saddle point (SP) when it rolls down from A, denoted by dotted line R3. For  $\alpha > \alpha_i$ , energy damping is too strong for the system to ‘climb’ over the saddle point, denoted by line R2. Value  $\alpha_i$  depends obviously on the magnetic field, and critical damping constant  $\alpha_c$  is the value of  $\alpha_i$  at  $h = h_{SW}$ .

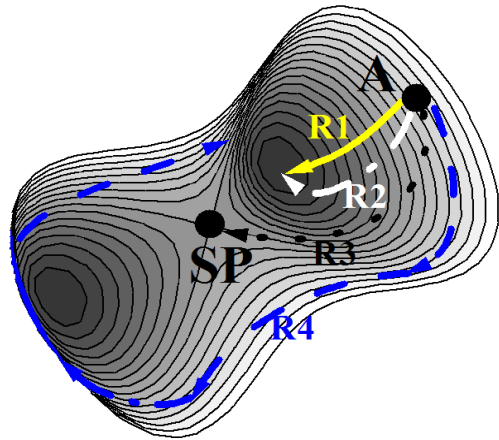


FIG. 3: (Color online) The schematic 3D energy landscape plot of the case  $h_1 < h < h_{SW}$ . Point A denotes the initial state, whose energy is supposed to be higher than that of the saddle point (SP). Lines R1, R2, R3 and R4 show schematically four typical evolution trajectories for  $\alpha = \infty$ ,  $> \alpha_i$ ,  $\alpha_i$ , and 0, respectively.

One may also understand the result from Fig. 4 of trajectories of various  $\alpha$  in the energy contour plot at  $h = h_{SW}$  along  $135^\circ$  to  $+x$ -axis. The result in the figure is for the uniaxial model with  $k_2 = 2$  and  $k_4 = 0$ . As mentioned early, the saddle point and one minimum merge together at  $h_{SW}$  to form an inflexion point denoted by T in Fig. 4. It is clear that all trajectories with  $\alpha > \alpha_c$  passing through the saddle-inflexion point while all those with  $\alpha < \alpha_c$  do not. One may notice that all curves of  $\alpha > \alpha_c$  do not move after they reach point T because T is a saddle point. But any small fluctuation will result in the system to leave T and to end up in FP.

In order to demonstrate the correctness of our reasoning of existence of  $\alpha_c$ , and the value of the critical damping constant varies with the magnetic anisotropy, we carried out numerical calculations on the uniaxial magnetic anisotropy model with different ratio of  $k_4/k_2$ . Fig. 5 is  $\alpha$ -dependence of the minimal switching field for  $k_4/k_2 = 0; 1/8; 1/4; 1/2$ , respectively. Indeed, all curves (depend only on the ratio of  $k_4/k_2$ ) saturate to their corresponding SW-limit values  $h_{SW}$  after  $\alpha$  is greater than certain values, the critical damping constants  $\alpha_c$ . Furthermore,  $\alpha_c$  is different for different  $k_4$ , varying from  $\alpha_c = 1$  for  $k_4 = 0$  to  $\alpha_c = 0.94$  for  $k_4 = k_2/2$ . Thus,  $\alpha_c = 1$  is not special at all!

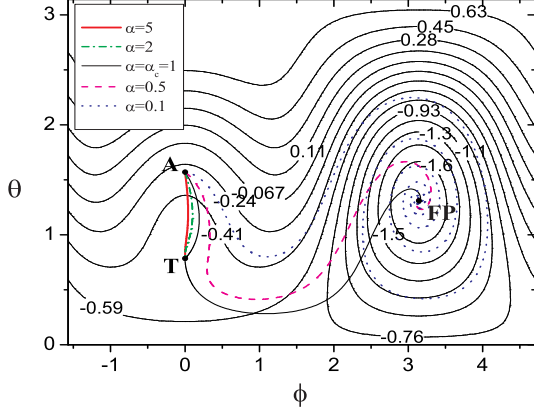


FIG. 4: (Color online) The contour plot of  $w(\phi, \theta)$  at  $h = h_{SW}$  for the uniaxial magnetic anisotropy model with  $k_2 = 2$  and  $k_4 = 0$ . The field is along  $3\pi/4$  to  $+x$ -axis. Point A is the initial point. FP denotes the stable fixed point. T denotes the inflexion point. All flow trajectories of  $\alpha \geq \alpha_c$  touch T while those with  $\alpha < \alpha_c$  do not.

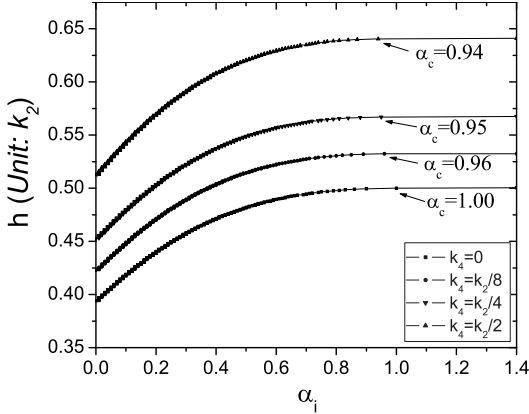


FIG. 5: The minimal switching field versus damping constant  $\alpha$ . The field is along  $3\pi/4$  to  $+x$  axis. Square:  $k_4/k_2 = 0$ ; Circle:  $k_4/k_2 = 1/8$ ; Down-triangle:  $k_4/k_2 = 1/4$ ; Upper-triangle:  $k_4/k_2 = 1/2$ . Smooth connection curves are to guide eyes.

### III.3 Changes of basins under an external field

We would like to investigate numerically how fixed points and their basins change under a field along different directions. In the following calculation,  $k_2 = 2$ ,  $k_4 = 0$ , and  $\alpha = 0.1$  is used. In the absence of an external magnetic field, there are two fixed points at  $(\theta = \pi/2, \phi = 0)$  and  $(\theta = \pi/2, \phi = \pi)$ , respectively. They are also the initial state (A) and the target state (B). Depending on the direction and strength of an applied field, two fixed points, FP1 and FP2, may move away from A and B. The numerical procedures are as follows: Divide the  $\theta - \phi$  plane ( $\theta \in (0, \pi)$ , and  $\phi \in (-\pi/2, 3\pi/2)$ ) into  $100 \times 50$  meshes. Each mesh site represents one particular state. Starting from an arbitrary state, the state

belongs to basin of FP1 (FP2) if the system evolves into fixed point FP1 (FP2) after a long enough time. Basin FP1 (FP2) is colored white (grey). Fig. 6-Fig. 8 are the basins with different external fields.

#### A. Field along the easy axis

Fig. 6 (a) is the basin without an external field. The basins divide the phase plane into two equal-area parts with the separatrix lines of  $\phi = \pi/2$  and  $3\pi/2$ . When a field parallel to the easy axis is applied, Points A and B are always two fixed points of the system. However the areas of their basins vary. Fig. 6 (b)-(d) show how the area of basin A shrinks while that of B expands as the field increases. When the field reaches the SW-limit (Fig. 6d), the area of basin A shrinks to zero. Thus B becomes the only stable fixed point and its basin is the whole phase plane when the field is above the SW-limit.

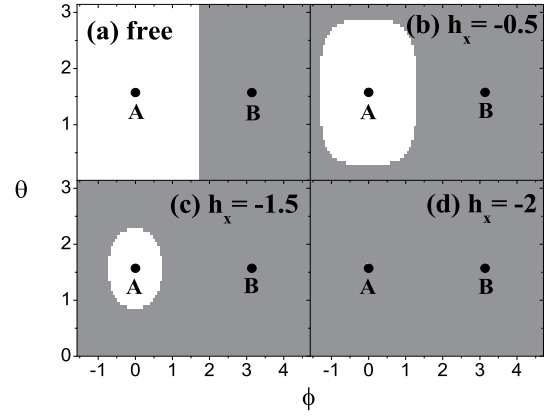


FIG. 6: The basins for  $k_2 = 2$ ,  $k_4 = 0$ , and  $\alpha = 0.1$  with various fields parallel to the easy axis. Points A and B, which are also the fixed points, are the initial and the target states. The white color is the basin of fixed point A and the grey color is that of B. (a) In the absence of an external field; (b)  $h_x = -0.5$ ; (c)  $h_x = -1.5$ ; (e)  $h_x = -2$  (SW-limit).

#### B. Field perpendicular to the easy axis

When a field perpendicular to the easy axis, say  $z$ -direction, is applied, the variations of the fixed points and basins are shown in Fig. 7. The positions of two fixed points shift along the  $\theta$ -axis, symmetrically located on the two sides of  $+z$ -axis. It is evident from Fig. 7 (a)-(c) that the basin shapes become layer-like structures. The outer parts of the basins become layers first. As the field increases, more basin areas become layers. However, the total areas of two basins are equal due to the symmetry of a perpendicular field when the field is below the SW-limit. When the field is higher than a certain value, point A will fall into the layered region (Fig. 7c) and may flow toward the right hand side of the phase plane. Once the magnetization passes the separatrix line ( $\phi = \pi/2$ ), it will evolve into the target state B if one can switch off the field. This precessional procedure was employed in experiments[11] and numerical calculations[13].



It is interesting to notice that the width of these layers become generally thinner when they are away from their cores (central parts of basins around fixed points), and the number of layers increases with the field. The width of a layer is determined by the size of basin core, energy variation in the phase plane, and the energy dissipation during a  $360^\circ$ -precession ( $\phi$  moves from  $-\pi/2$  to  $3\pi/2$ ). As the field increases, the areas of the core basins shrink, and the precession period is short as well. Thus layers become thinner while the layer number increases. The energy dissipating rate is  $\frac{dw}{dt} = -\frac{\alpha}{1+\alpha^2}|\vec{m} \times \vec{h}_t|^2$ . The precession period can be estimated as about  $(\vec{m} \times \vec{h}_t)^{-1}$  since  $\vec{m} \times \vec{h}_t$  is the angular frequency along the latitudes. So the energy loss is proportional to  $|\vec{m} \times \vec{h}_t| = |\vec{h}_t \sin \theta|$ , which is small for  $\theta$  is near  $\pi$ . Thus the width of the outer layers is thinner than that of inner ones. Fig. 7d shows when the field strength reaches SW-limit, the two fixed points merge to the same point  $\theta = 0$  (north-pole).

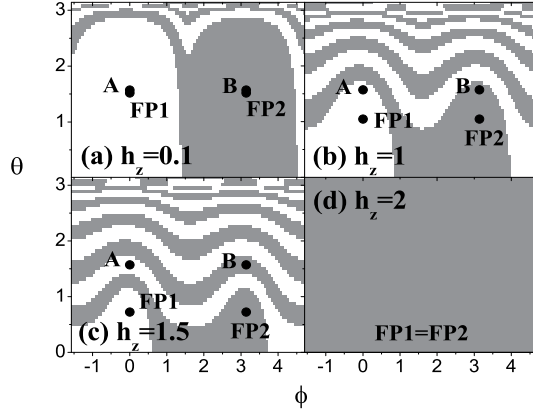


FIG. 7: The basins in the  $\theta$ - $\phi$  plane with different strength of a field perpendicular to the easy axis, say z-direction. Points A and B denote the initial and the target states. The white color is the basin for fixed point FP1 and the grey color is that for FP2. (a)  $h_z = 0.1$ ; (b)  $h_z = 1$ ; (c)  $h_z = 1.5$ ; (d)  $h_z = 2$  (SW-limit). Other parameters are the same as Fig. 6.

### C. Field at $135^\circ$ to the easy axis

We now investigate how the basins change under a field with  $135^\circ$  to the  $+x$ -direction since the minimal switching field is smallest around this direction[17]. Fig. 8 is the plot of fixed points and their basins at different field strengths. It has both features of cases with parallel and perpendicular fields. Increasing the field strength, the fixed points shall shift along  $\theta$ -axis while  $\phi$  does not change. Unlike the case of perpendicular field, the two fixed points have different  $\theta$  values. One can see that basin FP1 shrinks while that of FP2 expands as the field strength increases, a feature with parallel field. However, the layer structure also occurs in the outer parts of the basins. The stripes become thinner when the field increases and  $\theta$  is away from the fixed point. At the SW-

limit (Fig. 8d), the area of the basin of FP1 shrinks to zero.

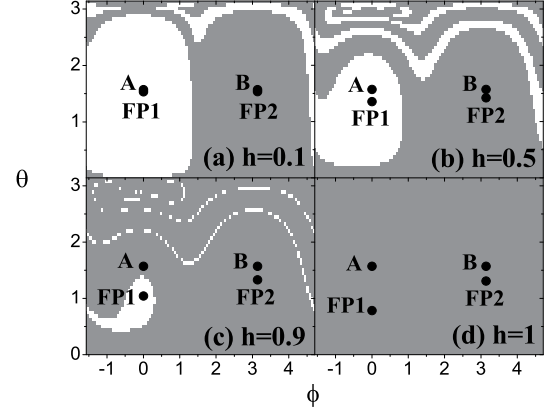


FIG. 8: The basins in  $\theta$ - $\phi$  plane with different  $h$  along  $135^\circ$  to the  $+x$  axis. Points A and B denote the initial and the target states. The white color is the basin for fixed point FP1 and the grey color is that for FP2. (a)  $h = 0.1$ ; (b)  $h = 0.5$ ; (c)  $h = 0.9$ ; (d)  $h = 1$  (SW-limit). Other parameters are the same as Fig. 6. It demonstrates that A and B could be connected by one phase flow trajectory in a field with both non-zero x- and z-components.

### III.4 Ballistic path

After seeing the change of fixed points and their basins under different field in the previous section, let us investigate the field and the reversal time for the ballistic connection. Without dissipation, LLG equation is a conservative system. A phase flow is an equipotential curve. As it was pointed out in Reference[19], only a perpendicular field is possible to connect the initial and the target states ballistically. Different from the conservative case[19], the system starting from A will never pass through the target state B in the presence of dissipation. Even under an infinitely large field, the energy loss during a  $180^\circ$  precession is not negligible. Although  $180^\circ$  precession time  $\tau$  decreases as inverse of magnetic field,  $\tau \sim \pi(1+\alpha^2)/h$  when  $h \gg 1$  and  $\alpha \ll 1$ , the energy dissipation rate goes as  $\frac{dw}{dt} = -\frac{\alpha}{1+\alpha^2}|\vec{m} \times \vec{h}_t|^2 \propto h^2$ , thus the energy loss during  $\tau$  is proportional to  $h$  field[24]! In order to connect both A and B ballistically, one has to create a small energy difference between A and B such that the energy dissipated on its way from A to B equals the energy difference.

On the other hand, Eq. (3) can be solved exactly in the absence of magnetic anisotropy ( $k_2 = 0$ ,  $k_4 = 0$ )[22] with solution  $\phi = ht/(1+\alpha^2)$  and  $\cos \theta = [(1+\cos \theta_0)e^{2\alpha ht/(1+\alpha^2)} - 1 + \cos \theta_0]/[(1+\cos \theta_0)e^{2\alpha ht/(1+\alpha^2)} + 1 - \cos \theta_0]$ , where  $\theta_0$  is the initial angle between the field and the magnetization (we assume the field is along the z-axis and the initial  $\phi$  is zero). Thus the ballistic reversal

corresponding to apply a field along direction  $\theta$  satisfying  $-\cos\theta = [(1 + \cos\theta)e^{2\alpha\pi} - 1 + \cos\theta]/[(1 + \cos\theta)e^{2\alpha\pi} + 1 - \cos\theta]$ . It is interesting to notice that the solution is unique and the angle is  $\tan(\theta/2) = e^{\alpha\pi/2}$ .

Given a damping constant  $\alpha$  and magnetic anisotropy, described by  $k_2$  and  $k_4$ , the  $180^\circ$  precession time  $\tau(h, \beta)$  is a function of field strength  $h \equiv \sqrt{h_x^2 + h_z^2}$  and its angle  $\beta$  to the z-axis ( $\beta$  relates to  $\theta$  by  $\theta = \pi/2 + \beta$ ). Thus the energy dissipated  $\Delta\epsilon(h, \beta) = \int_0^\tau \frac{dw}{dt} dt$  during  $\tau$  is also a function of  $h$  and  $\beta$ . For  $h \gg 1$ , one can neglect the magnetic anisotropy, and above isotropic solution should be good. Under the limit,  $\Delta\epsilon$  is  $2h[1/(1 + \tan^2(\beta/2 + \pi/4))e^{-2\alpha\pi} - 1/(1 + \tan^2(\beta/2 + \pi/4))]$ . The energy difference  $\Delta E(h, \beta)$  between A and B is  $2h \sin(\beta)$ . Therefore, a ballistic path must satisfy  $\Delta\epsilon = \Delta E$  (a necessary condition but not a sufficient one). Due to the symmetric reason, one needs to consider only  $\beta \in (0, \pi/2)$ . Without energy dissipation, the only solution is  $\beta = 0$  and any  $h$  larger than certain minimal value. With large field ( $h \gg 1$ ) and energy dissipation ( $\alpha \neq 0$ ), the approximate solution is  $\tan(\beta/2 + \pi/4) = e^{\alpha\pi/2}$ , the same as the isotropic solution  $\tan(\theta/2) = e^{\alpha\pi/2}$ . For  $\alpha \neq 0$  and  $k_2 \neq 0$ , we cannot solve  $\Delta\epsilon = \Delta E$  analytically. The field configuration of the ballistic connection between A and B was found numerically. The results were displayed in Figure 9.

Surprisingly, the field can be applied in a range of direction, i.e. a direction window. Given a  $\beta$  in this direction window,  $h$  is uniquely determined. Both the lower and the upper bound of this  $\beta$ -window increase with the damping constant. Figure 9a is the plot of the upper and the lower bounds of  $\beta$  as a function of  $\alpha$ . The solid line is  $\tan(\beta/2 + \pi/4) = e^{\alpha\pi/2}$ . Indeed, the window is around the solid line. The width of the window depends both on the damping constant and the magnetic anisotropy. At the zero and the infinite damping constant, the width is zero. It is also zero in the absence of magnetic anisotropy as illustrate by the exact solution mentioned in the early paragraph. Thus, the width is expected to oscillate with  $\alpha$  for a given magnetic anisotropy. This oscillation was indeed observed in numerical calculations as shown in Fig. 9b for  $k_2 = 2$ ,  $k_4 = 0$ . The upper-left inset of Fig. 9b is the field and the corresponding reversal time in the direction window for  $\alpha = 0.1$  and  $k_2 = 2$ ,  $k_4 = 0$ . In this particular case,  $\beta$  is between 0.134 and 0.156. One sees that  $h$  increases while reversal time decrease with  $\beta$ . The similar plot for  $\alpha = 1$  is shown in the lower-right inset of Fig. 9b. Opposite to the case of small  $\alpha$  ( $= 0.1$ ),  $h$  decreases and reversal time increases with  $\beta$ . Thus one should compare the lower bound for  $\alpha < 0.57$  and the upper bound for  $\alpha > 0.57$  with  $\tan(\beta/2 + \pi/4) = e^{\alpha\pi/2}$  since it is expected to be exact for  $h \rightarrow \infty$  when the magnetic anisotropy can be neglected. An excellent agreement was shown in Fig. 9a. Fig. 9b is the window width  $\Delta\beta$  as a function of  $\alpha$ . Our numerical results indicate that the perpendicular configuration employed in the current

experiments[11, 12] cannot achieve a fully ballistic reversal. It should be pointed out that above results are for the precise ballistic magnetization reversal. As we mentioned early, other field can also switch magnetization if one will also like to use the ringing effect at certain stages during the reversal process.

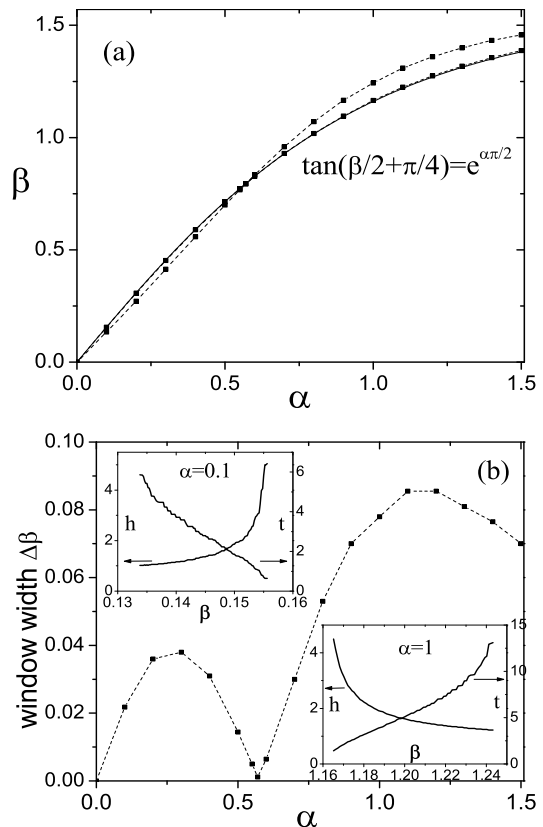


FIG. 9: (a) The upper and lower bounds of  $\beta$  as a function of damping constant  $\alpha$ . The solid line is  $\tan(\beta/2 + \pi/4) = e^{\alpha\pi/2}$ , which should be compared with the upper bound of  $\beta$  for  $\alpha < 0.57$  and the lower bound for  $\alpha > 0.57$ . The magnetic anisotropy is  $k_2 = 2$  and  $k_4 = 0$ . (b) The window width  $\Delta\beta$  vs.  $\alpha$  for  $k_2 = 2$  and  $k_4 = 0$ . Insets: the magnetic field and the corresponding reversal time as a function of  $\beta$  in the ballistic direction window.  $\beta \in (0.134, 0.156)$  for  $\alpha = 0.1$  (upper-left inset),  $\beta \in (1.165, 1.243)$  for  $\alpha = 1$  (lower-right inset). The dashed lines are used to guide eyes.

### III.5 Discussions

The SW theory is a classical work[10] which is based on the energy consideration. Its connection to the LLG theory was not discussed in literatures. We clarify that the SW theory is the infinite dissipation limit of the LLG. Under the limit, the magnetization moves along the steepest energy descent path. The discrepancy between the SW-limit and the numerical minimal switching field has been known for many years[17]. Also, the exist-



tence of a critical value of  $\alpha$  was known numerically[17]. But its original was not given in the previous theoretical studies[13, 14, 17, 18, 19]. To the best of our knowledge, its meaning is first revealed now.

So far we have reformulated the magnetization reversal in terms of the language of nonlinear dynamics. The conventional reversal technique is to make the target state to be the only fixed point while the fast switching method is to connect the initial and the target states on the same phase flow trajectory. Dissipation and magnetic anisotropy play very interesting roles in a ballistic magnetization reversal. Without dissipation, only perpendicular fields larger than a minimal switching field can create a ballistic path between the initial and the target states. In the absence of a magnetic anisotropy and  $\alpha \neq 0$ , field direction is not perpendicular but unique, and the field magnitude is arbitrary. In the presence of both dissipation and anisotropy, allowed directions for the ballistic connection form a window. But inside the window, the field magnitude is single valued. Due to the energy dissipation, applying a perpendicular field to the easy axis of a uniaxial Stoner particle cannot directly connect initial and final states by a phase flow trajectory. Thus, the configuration employed in the current fast magnetization reversal experiments[11, 12] is not the best one. A proper field along the direction window can improve the best experimental numbers up to now.

There are advantages and disadvantages for the conventional and the fast reversal methods. Although the switching time in the conventional technique is at the nanoseconds, the technology is less demanding and easy to implement. On the other hand, the fast switching method could make the switching time at picoseconds scale, but it needs to have precise control of the magnetic pulse. If it is implemented, the cost should be much higher than that of the conventional one. Besides time issue, minimal switching field is another concern. The minimal switching field in the conventional reversal technique occurs when only one energy minimum exists in the basin of the final state. Depending on the dissipation rate, the minimal field in the precessional fast switching method may not be much smaller than the SW-limit. So far, in both conventional and fast magnetization reversal schemes, both the direction and the magnitude of the magnetic field during the pulse duration are assumed to be fixed. If the direction of the magnetic field is allowed to vary with time, the minimal switching field can be even smaller. However it will be more demanding to implement technologically.

#### IV. CONCLUSION

In conclusion, we show that the magnetization reversal can be conveniently examined in the terminology of nonlinear dynamics. The presence of the dissipation will not

fail the fast switching method. We clarify that the SW result is the limit of LLG theory with an infinitely large dissipation. In this limit, the magnetization moves along the steepest energy descent path. We show that there is a critical value of the damping constant for a given magnetic anisotropy, above which, the minimal switching field is the same as the prediction of SW theory. Based on the change of fixed points and their basins under an external field in different directions, we show that the magnetization reversal time can be much shorter when the field drives both initial and target states away from fixed points, but puts them on the same phase flow trajectory. In the absence of energy dissipation, the field should be applied perpendicularly to the easy axis in order to achieve a ballistic magnetization reversal. However, with both energy dissipation and a magnetic anisotropy, the field can be applied along a direction window. The width of the window depends on both the damping constant and the magnetic anisotropy. It is zero for either zero damping constant or zero magnetic anisotropy ( $k_2 = 0$  and  $k_4 = 0$ ). Unlike the conventional magnetization reversal method, the new scheme demands a precise control of picoseconds pulse of a magnetic field.

#### ACKNOWLEDGMENTS

We would like to thank D. Xiao and Q. Niu for sending us their preprint before submitting for publication. This work is supported by UGC, Hong Kong, through RGC CERG grants.

- 
- [1] Robert C. O'handley, *Modern Magnetic Materials: Principles and Applications*, (John Wiley & Sons, New York, 2000).
  - [2] Shouheng Sun, C. B. Murray, D. Weller, L. Folks, and A. Moser, *Science* **287**, 1989 (2000).
  - [3] C. T. Black, C. B. Murray, R. L. Sandstrom, and Shouheng Sun, *Science* **290**, 1131 (2000).
  - [4] S. I. Woods, J. R. Kirtley, Shouheng Sun, and R. H. Koch, *Phys. Rev. Lett.* **87**, 137205 (2001).
  - [5] D. Zitoun, M. Respaud, M.-C. Fromen, M. J. Casanove, P. Lecante, C. Amiens, and B. Chaudret, *Phys. Rev. Lett.* **89**, 037203 (2002).
  - [6] B. Hillebrands and K. Ounadjela, eds., *Spin Dynamics in Confined Magnetic Structures I & II*, (Springer-Verlag, Berlin, 2001).
  - [7] W. K. Hiebert, A. Stankiewicz, and M. R. Freeman, *Phys. Rev. Lett.* **79**, 1134 (1997).
  - [8] Y. Acremann, C. H. Back, M. Buess, O. Portmann, A. Vaterlaus, D. Pescia, and H. Melchior, *Science* **290**, 492 (2000).
  - [9] T. M. Crawford, T. J. Silva, C. W. Teplin, and C. T. Rogers, *Appl. Phys. Lett.* **74**, 3386 (1999).
  - [10] E. C. Stoner, and E. P. Wohlfarth, *Phil. Trans. Roy. Soc. London* **A240**, 599 (1948), reprinted in *IEEE Trans.*

- Magn. **27**, 3475 (1991).
- [11] C. H. Back, D. Weller, J. Heidmann, D. Mauri, D. Guarisco, E. L. Garwin, and H. C. Siegmann, Phys. Rev. Lett. **81**, 3251 (1998); C. H. Back, R. Allenspach, W. Weber, S. S. P. Parkin, D. Weller, E. L. Garwin, and H. C. Siegmann, Science, **285**, 864 (1999).
  - [12] H. W. Schumacher, C. Chappert, P. Crozat, R. C. Sousa, P. P. Freitas, J. Miltat, J. Fassbender, and B. Hillebrands, Phys. Rev. Lett. **90**, 017201 (2003); H. W. Schumacher, C. Chappert, R. C. Sousa, P. P. Freitas, and J. Miltat, Phys. Rev. Lett. **90**, 017204 (2003).
  - [13] L. He, and W. D. Doyle, J. Appl. Phys. **79**, 6489 (1996).
  - [14] M. Bauer, J. Fassbender, B. Hillebrands, and R. L. Stamps, Phys. Rev. B **61**, 3410 (2000).
  - [15] Y. Acremann, C. H. Back, M. Buess, D. Pescia, and V. Pokrovsky, Appl. Phys. Lett. **79**, 2228 (2001).
  - [16] J. Miltat, G. Albuquerque and A. Thiaville, in *Spin Dynamics in Confined Magnetic Structures I*, edited by B. Hillebrands and K. Ounadjela (Springer-Verlag, Berlin, 2001).
  - [17] L. He, W. D. Doyle, and H. Fujiwara, IEEE. Trans. Magn. **30**, 4086 (1994).
  - [18] D. G. Porter, IEEE. Trans. Magn. **34**, 1663 (1998).
  - [19] Di Xiao, and Qian Niu, cond-mat/0409671.
  - [20] Textbooks on nonlinear physics, such as, S. H. Strogatz, *Nonlinear Dynamics and Chaos*, (Addison-Wesley, 1994).
  - [21] L. Landau, and E. Lifshitz, Phys. Z. Sowjetunion **8**, 153 (1953); T. L. Gilbert, Phys. Rev. **100**, 1243 (1955).
  - [22] R. Kikuchi, J. Appl. Phys. **27**, 1352 (1956).
  - [23] P. R. Gillette, and K. Oshima, J. Appl. Phys. **29**, 529 (1958).
  - [24] One cannot use a small  $h$  to switch a magnetization in the presence of a non-zero magnetic anisotropy. A finite  $h$  is needed in order to overcome the potential barrier along a reversal path.